PJRT
Fall 2017

Anica Bulic – Ablation

Chalese Richardson - Devices

Louis Rigos – CV Genetics

William Goodyer – Basic Science

Initial international multicenter human experience with a novel epicardial access needle embedded with a real-time pressure/frequency monitoring to facilitate epicardial access: Feasibility and safety

Di Biase L, Burkhardt JD, Reddy V *et* al. Heart Rhythm 2017; 14:981-988.

Background: Percutaneous epicardial access is an alternative approach for mapping and ablating difficult supraventricular and ventricular tachyarrhythmias. The subxiphoid approach is the most frequently used with the most significant risk being inadvertent RV free wall perforation leading to pericardial tamponade (reported incidence 3.7 – 10%). This has led to recent efforts at improving device design in order to improve procedural safety. Epicardial procedures were originally performed using 17- to 18-G Tuohy needles, and most recently a 21-G micropuncture needle with/without a short 18-G needle ("needle-in-needle" technique). The EpiAccess System was designed to allow the same procedural technique as with the Tuohy needle while incorporating a fiber optic sensor in the needle tip to display real-time pressure waveform to help confirm location. This multicenter international registry sought to assess the feasibility and safety of the EpiAccess System in patients undergoing epicardial access for various procedures.

Summary: 25 patients were prospectively enrolled (76% male; average age ~ 62 yrs, range 28-84 yrs; indication was VT ablation in 80% and Lariat LAA occlusion device deployment in 20%). An anterior approach was attempted in all cases with a 100% success rate and an average procedural time of 4.4 min +/- 1.6 min. There was no statistical difference between experienced and non-experienced operators, defined as 2 or less epicardial punctures in their career. 1 unintended RV puncture and pericardial effusion >80mL. No tamponade or death.

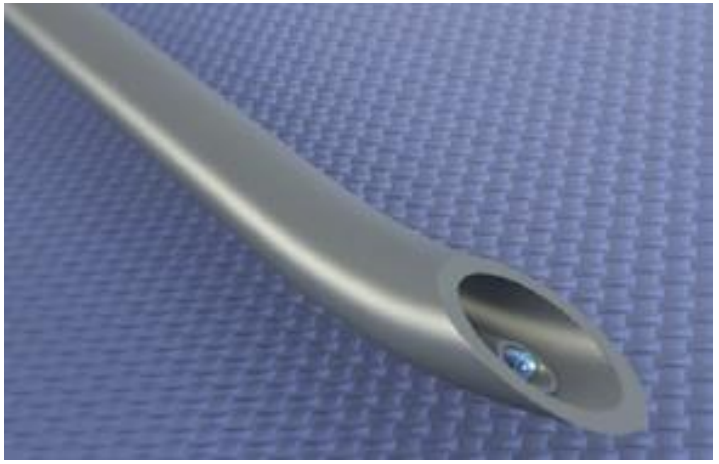

Figure 1. Access needle (6Fr, 12.6 cm) with a pressure frequency fiber optic sensor within a stainless steel tube, welded inside the lumen of the cannula.

Previous studies have compared the safety of MP to Tuohy needles and have reported an incidence of large pericardial effusion of 0.8% vs. 8.1%, respectively, and inadvertent myocardial puncture of 7.6% vs. 6.8%, respectively.

Subxiphoid Epicardial Access Technique:

- Needle entry is 2-3 cm below and slightly lateral to xiphoid process, with the bevel of the needle pointed upward and rightward in an anterior approach.
- Needle is directed to the mid left clavicle and oriented to the left border of the subxiphoid process and the left rib.
- Needle is advanced slowly under fluoroscopic guidance as it passes subcutaneous tissue and above the dome of the diaphragm.
- Apply gentle pressure over epigastrium to steer left lobe of liver, gastric fundus, and in some cases the transverse colon, away from the path of the needle.
- Once over dome of the diaphragm (i.e. behind sternum), the steep of the needle is angled at 30-45 degrees.
- As the needle is advanced, the pressure frequency signal detects extrapericardial, pericardial and ventricular transitions. Fluoroscopy is used to confirm position.
- Transition from extrapericardial to pericardial space is detected with a change in the pressure signals from inconsistent low amplitude signals to consistent pulsatile signals of +/- 5mmHg. Confirm position with contrast injection, outlining pericardial space.
- A long guidewire is advanced into the pericardial space and in the LAO view it follows the left cardiac border and crosses from left to right side in front of great vessels.
- A long sheath is advanced into the pericardial space, through which mapping/ablation catheters are introduced.

Pediatric Implications:

The pediatric implications remain to be seen. There could be a potential role for epicardial access in difficult SVT/VT ablations in the ACHD population and select pediatric patients.

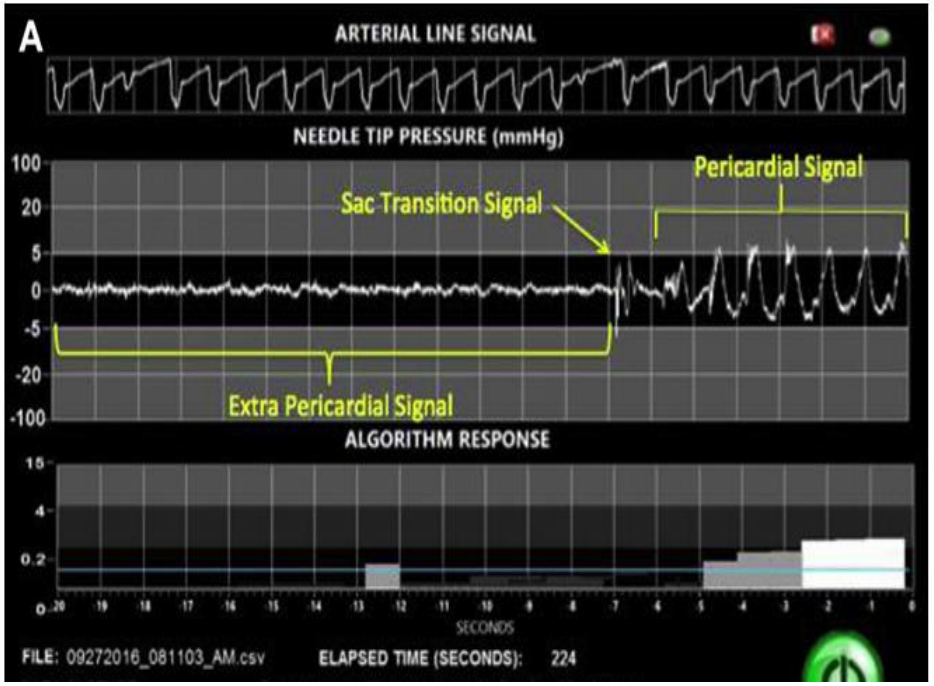

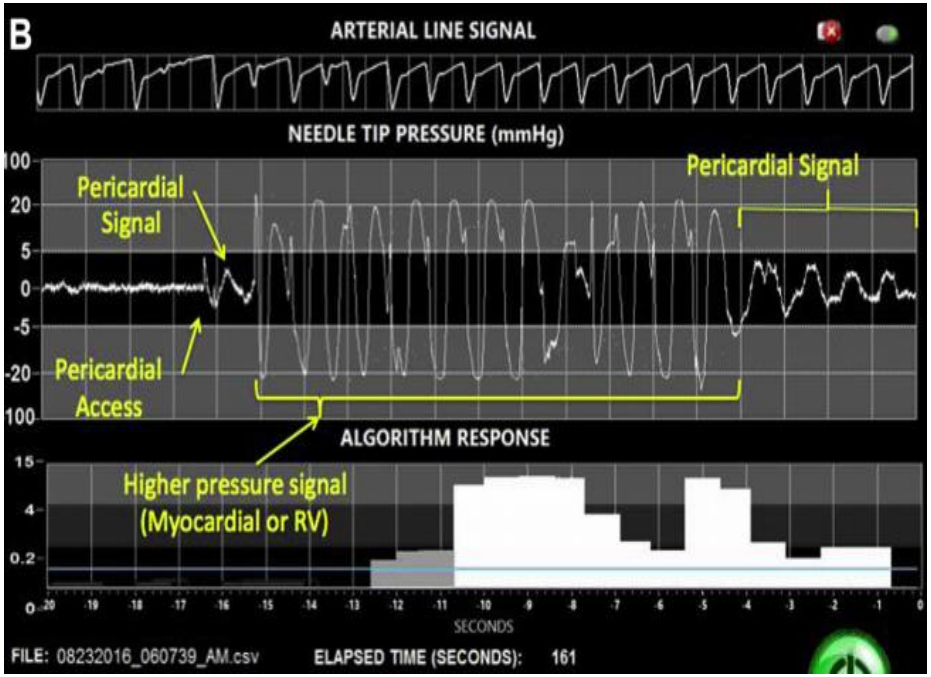

Comparison of strategies for catheter ablation of focal atrial tachycardia originating near the His bundle region

Lyan E, Toniolo M, Tsyganov A *et* al. Heart Rhythm 2017; 14:998-1005.

Background: Radiofrequency ablation of para-Hisian atrial tachycardia (AT) confers a risk of complete heart block due to its proximity to the AV node. Several studies suggest that these atrial tachycardias can be successfully ablated from the RA, LA, and noncoronary cusp (NCC) of the aortic valve. However, there is little data comparing these different ablation strategies to each other.

Summary: This retrospective multicenter study included 68 patients (72% F, mean age 61 +/-13 yrs) with para-Hisian AT who underwent mapping in the RA/LA/NCC during AT before RFA. Activation mapping was done conventionally in 38% and with 3D electroanatomical mapping in 62%. Initially the RA was mapped and when the AT was localized to the para-Hisian region, further detailed mapping of the LA via a transseptal approach and/or mapping of the NCC through a retrograde approach was done at the operator's choice. Their results showed that AT ablation in the NCC was the most successful at terminating AT with less RF lesions, no transient or permanent second/third degree HB, and a low recurrence rate (mean follow-up 33.5 +/- 25.4 months).

Table 2 Mapping and ablation data for each patient in the study

Variable	RA	LA	NCC	*P*
No. of cases with ablation	28	16	52	NA
Local activation time (ms)	0	2.6 ± 9.8	−7 ± 16.8	<.05
Mean AoP (ms)	−42.5 ± 15.4	−28.3 ± 18.3	−49.8 ± 17.3	<.05
Mean Adur (ms)	50.8 ± 15.9	43.0 ± 7.4	50.0 ± 14.2	.78
No. of RF applications	5.2 ± 4.4	7.5 ± 2.7	3.2 ± 1.7	<.05
Successful ablation	13 (46.4)	4 (25.0)	46 (88.5)	<.05
Transient AVB	3 (10.7)	1 (6.3)	0	NA
Permanent second- or third-degree AVB	4 (14.3)	0	0	NA
Prolongation of AH (after ablation) (ms)	14.6 ± 21.7	2.3 ± 5.6	2.3 ± 10.6	<.05
Prolongation of HV (after ablation) (ms)	0.5 ± 5.0	−0.9 ± 1.9	0.2 ± 2.0	.69
Use of 3D mapping system	16 (57.1)	14 (87.5)	31 (59.6)	<.05
Use of ICE	7 (25.0)	8 (50.0)	13 (25.0)	<.05
Use of irrigated-tip catheter	12 (42.9)	16 (100)	24 (46.2)	<.05
Recurrences during follow-up	5 (38.5)	1 (25)	2 (4.4)	<.05

Activation mapping: Correlation of 3D electroanatomical mapping with fluoroscopy (B) and intracardiac echocardiogram (C). The earliest activation site in the RA was at the His bundle (His 3-4). Local activation time (LAT) is the time difference b/t the earliest RA activation at His 3-4 and the local EGM on the ablation catheter (MAP 1, 1-2, 3-4). LAT and the timing of the onset of the P wave on surface ECG were used to define the earliest activation site (EAS).

Implications: The NCC approach to ablating para-Hisian atrial tachycardias may be considered a viable mapping/ablation strategy. However, further studies comparing cryoablation (with a lower risk of AV block) to the NCC approach in children would be helpful.

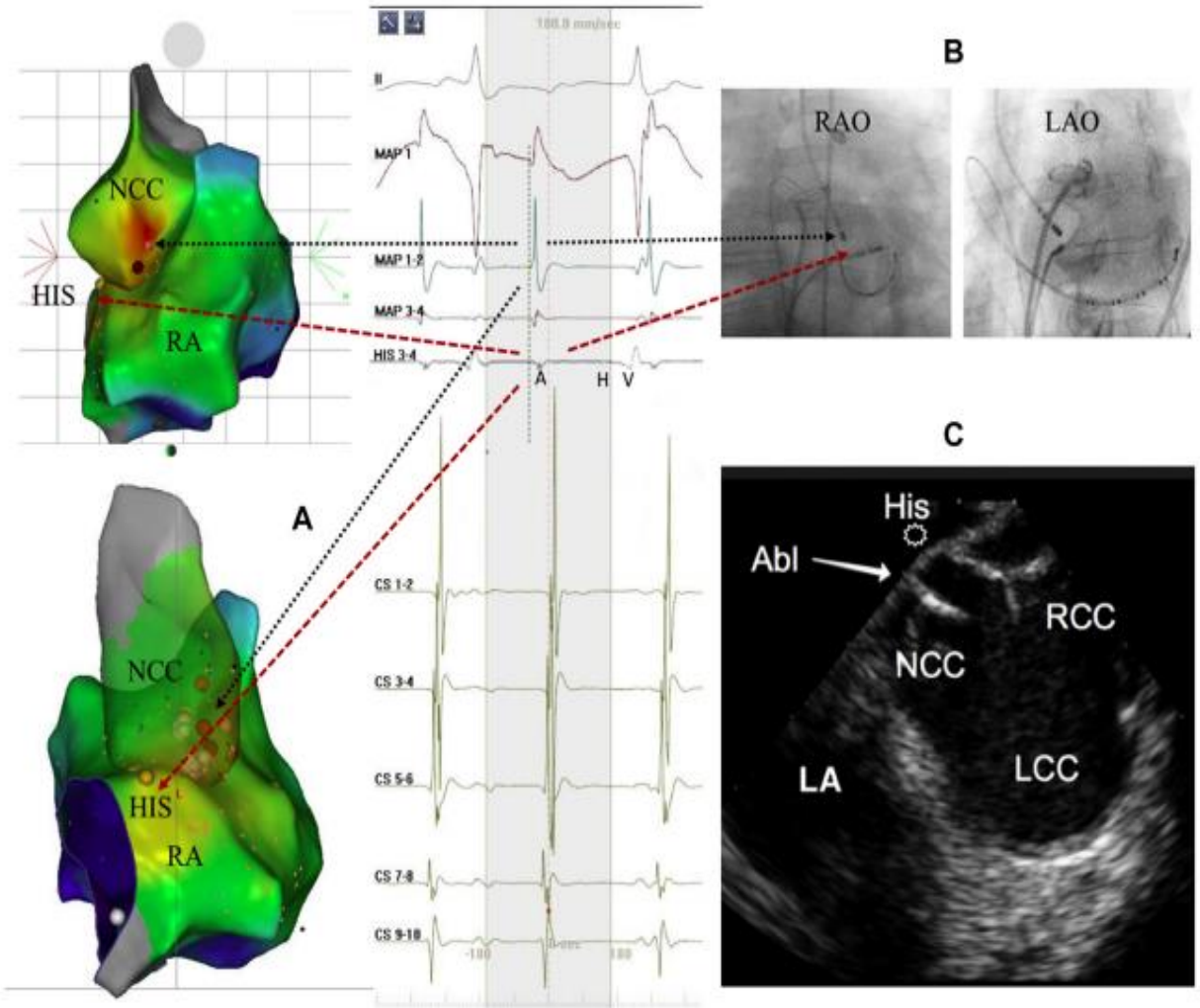

Leadless Pacemakers: practice and promise in congenital heart disease

Journal of Congenital Cardiology, July 2017, Volume 1, Issue 4: 1-6. DOI 10.1186/s40949-017-0007-5
Clarke TSO, Zaidi AM and Clarke B

Background: Leadless pacemakers offer a possible solution to some of the challenges faced with transvenous devices in patients with congenital heart disease and venous abnormalities, anatomical anomalies and access issues. They may also help address some of the more common long-term complications associated with both transvenous and epicardial leads, including lead fractures and longevity.

Objectives: This review article discusses early study data on two leadless pacemakers and compares the data on each device and to conventional transvenous pacing systems.

Results: The two leadless pacemakers on the market are the Nanostim™ LP, St. Jude Medical and the Medtronic Micra™ TPS. Both are currently only able to pace in VVIR mode and are MRI –conditional. Early studies have shown on significant decrease in infection risk compared to transvenous and epicardial leads. The Nanostim™ showed a higher risk of perforation when compared to the Micra™ . The Micra™ had higher risk of dysrhythmia and vascular complications, likely due to the size of delivery system. Overall serious adverse events have been less with the Nanostim™ (6.7%) when compared to both transvenous and epicardial lead placement combined(10%) and the Micra™ (18.6%).

Conclusion: Leadless pacemakers may have potential for use in the pediatric congenital heart population but more longer follow up data is needed.

Comments: Although promising, some significant limitations in the pediatric and CHD populations include the the size of the delivery sheath required for deployment, limited indications for VVI pacing and limited follow-up to predict battery longevity. Another important limiting factor may be ease of retrievability which is not yet known given the size of pediatric hearts when compared to adults. Device abandonment and placement of subsequent devices may not be an option in this population.

Nanostim ™LP, St. Jude Medical

- 42mm x max 5.99mm
- Active fixation: 1° helical screw–in, 2° nylon tines
- Delivery: Fem V 16 F – 18 F
  - Initially to RV apex but revised to Apical septum
- Interrogation: New system using surface electrodes with wireless St. Jude Medical Programmer
- Remote monitoring: Pending on Merlin ™
- Early study data:
  - » n = 300
  - » Implant success: 95.7%
  - » Serious Adverse Events (n = 300, total 6.7%)
    - Dislodgement: 1.7%
    - Cardiac perforation: 1.3%
    - Elevated pacing thresholds: 1.3%
    - Vascular complications: 1.3%
    - Other: 1.1%

Fig. 1 Nanostim LP Leadless pacemaker (St Jude Medical)

Micra™ TPS, Medtronic

- 25.9mm x 6.7mm
- Passive fixation: 4 protractible nitinol tines
- Delivery: Fem V 23 F internal/ 27 F outer diameter
- Interrogation: Medtronic 2090 programmer/programmer head
- Remote monitoring: Pending on Carelink
- Early study data
  - » n = 140
  - » Implant success: 100%
  - » Serious Adverse events (18.6%)[1]
    - Dysrhythmias: 6.4%
    - Vascular complications: 6.3%
    - Cardiac perforation: 0.7%
    - Vasovagal syncope: 1.4%
    - Angina pectoris: 1.4%
    - Other: 2.4%
      - Acute MI (0.7%)
      - Pericardial effusion (0.7%)
      - Pericarditis (0.7%)

Fig. 2 Medtronic Micra transcatheter pacing system (TPS)

1. Ritter P, Duray GZ, Steinwender C et al. Early performance of a miniaturized leadless cardiac pacemaker: the Micra Transcatheter Pacing Study. Eur Heart J. 2015. (Epub ahead of print).

Minimally invasive epicardial implantable cardioverter-defibrillator placement for infants and children: An effect alternative to the transvenous approach

Heart Rhythm Society, September 2016, Volume 13, No 9: 1905-1912
http://dx.doi.org/10.1016/j.hrthm. 2016.06.024
Schneider AE, Burkart HM, Ackerman MJ, Dearani JA, Wackel P, Cannon BP

Background: Transvenous ICDs pose a risk of venous occlusion or TR which, and theses risks are not present with epicardial ICDs.

Objective: To evaluate the results of minimally invasive epicardial ICD lead placement in children.

Methods: Single center, retrospective chart review from 1/2011 – 12/2015 of patients < 18 years undergoing epicardial ICD placement. Minimally invasive technique described as a mini-anterior thoracotomy using a left sided 2-3 cm inframammary incision (vs. standard subxyphoid incision of 7-8 cms).

Results: A minimally invasive approach taken in 28/40 patients (61%) with follow up of 2 ± 1.3 years. Complications occurred in 6 of those patients (15%) including pleural effusions, pneumothorax requiring chest tube and superficial soft tissue infection. Due to occurrence of pleural effusions (n=3) early in the study, subsequent patients (n=25) were treated prophylactically with daily furosemide and ibuprofen TID for 7-10 days with no further development of effusions. 56/58 (97%) appropriate shocks were successful on the 1st attempt. Four patients (9%) received 34 total inappropriate shocks due to lead fractures or micro fractures.

Conclusion: Minimally invasive epicardial ICDs may have an increased cosmetic benefit over traditional thoracotomy or sternotomy and offer an alternative to transvenous approach especially in patients < 6 years old.

Comments: The study was limited by short follow up period with potential underestimation of lead and/or system failures. The small sample size also limits study power and possible generalizability.

Lidocaine attenuation testing: An *in vivo* investigation of putative LQT3-associated variants in the SCN5A-encoded sodium channel

Heart Rhythm, Vol 14 No 8 August 2017

Heather Andersen, J. Martijn BOS, Jaime D. Kapplinger, Jana M. Meskill, Dan Ye, Michael J. Ackerman

Background: Long QT syndrome (LQTS) is an inherited disorder (1:2000) characterized by abnormal ventricular repolarization that can precipitate ventricular arrhythmias . Approximately 5-10% of LQTS is caused by gain-of-function mutations in the *SCN5A*-encoded sodium channel and termed LQTS type 3. Causative mutations result in either a delay of sodium channel inactivation, increased late sodium current, or increased window current. There have been many mutations in the SCN5A associated with LQT3 and it remains essential in identifying those that are disease causing. Approximately 2% of healthy individuals carry rare variants of the SCN5A making interpretation, disease management, and screening challenging. Lidocaine attenuation testing (LAT) has been shown to have a sensitivity of 88% and specificity of 100% for the diagnosis of LQTS based on QTc duration changes; however its use for provocative testing among patients with the LQT3 subtype is unknown.

Objective: To describe the results of LAT in patients with suspected LQT3 and correlate those results with phenotype and pathogenicity of SCN5A variants to evaluate the use of LAT to distinguish true LQT3-causing mutations from ambiguous variants.

Methods: Retrospective, single center study, 2002-2013, mean age 22 ± 11 years. Patients with possible or probable SCN5A-LQT3 who underwent LAT **(n=25).** All measurements obtained from Lead II. LAT considered Positive: ≥ 30 ms QTc interval shortening from baseline at any time point during the infusion. (Refer to table A). In vitro results, variant classification, and clinical phenotype (Schwartz score) were compared to the LAT results. Mean baseline QTc interval was 459 ± 30 ms. No patients had any events prior to diagnosis. 17 patients (68%) had a family history of LQTS (48%) or sudden cardiac death (48%). Thirteen SCN5A variants were detected.

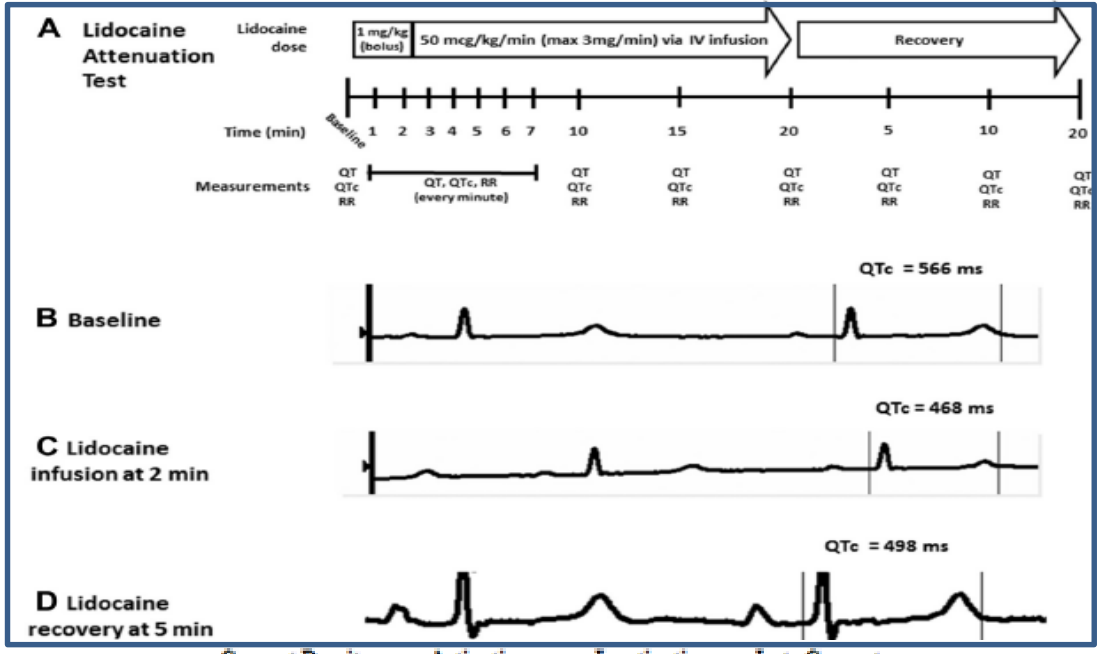

RESULTS: A positive LAT correlated in 86% of cases with in vitro evidence of abnormal channel function (refer to table B) with a mean QTc shortening of 43 ms compared to 25 ms for variants with wild-type function status resulting in a sensitivity of 81% and specificity of 71%. Using a combination of *in vitro* results and variant classification there was a PPV 85% and NPV of 67%. Patients with a positive LAT tended to have a higher Schwartz Score, but not statistically significant due small sample size.

SCN5A Variants	Current Density % change	Activation $V_{1/2}$ Shift (mV)	Inactivation $V_{1/2}$ Shift (mV)	Late Current % Change	LAT test
E48K	-37	+4*	-3	+0	Positive
R190Q	-8	0	+1	+21	Negative
L461V	N/A	N/A	N/A	N/A	Negative
E462A	-9	-3	+1	-5	Negative
G615E	-6	+1	+2	-	Negative/Positive
R800L **	-37*	-1	+2	+26	Positive
T1304M**	-45*	-4	-1	-8	Positive
M1320V	+8	+1	+2	+63	Negative
N1325S**	N/A	-6*	-3	Increase	Positive
R1644H**	N/A	+2	+2	Increase	Positive
E1784K**	-30	+6	-3	+243*	Negative/Positive

Significance: Lidocaine attenuation provides a provocative test for evaluating LQTS and risk stratification. LAT cut off values will impact SCN5A variants deemed clinically significant with more data needed to determine normative values for incurred QTc changes. The correlation between genotype and phenotypic response is complicated by other factors not well described. Positive predictive and negative predictive values similar to exercise/epinephrine testing in LQT1/LQT2. LAT can provide information about potential presence of pathogenic Na channel function and allow for pre-genetic test result and earlier initiation of therapy.

The QUIDAM study: Hydroquinidine therapy for the management of Brugada syndrome patients at high arrhythmic risk

Heart Rhythm, Vol 14, No 8, August 2017

Antoine Andorin, Jean-Baptiste Gourraud, Jacques Mansourati, Swanny Fouchard, Herve le Marec, Phillipe Maury, Phillipe Mabo, Jean-Sylvain Hermida, Jean-Claude Deharo, Beatrice Delasalle, Simon Esnault, Nicholas Sadoul, Jean-Marc Davy, Antoine Leenhardt, Didier Klug, Pascal Defaye, Dominique Babuty, Frederic Sachler, Vincent Probst

Background: Brugada syndrome (BrS) is an inheritable genetic disease that is associated with sudden cardiac death in apparently healthy individuals. Since its first description many advancements have been made in our understanding of the pathophysiology as well as attempts to risk stratify. However, management options are limited and remain dependent on an implantable cardioverter-defibrillator (ICD) with a high rate of complications. Despite ICD being the mainstay of treatment it does not reduce life-threatening ventricular arrhythmias. Much debate remains around the use of Hydroquinidine (HQ) (class 1A) in preventing life-threatening ventricular arrhythmias despite its long standing established safety and efficacy. Aside from its blocking effects of I_{Kr} and I_{Na} , HQ has been shown to block I_{to} . The transmural heterogeneity of I_{to} has been shown to induce repolarization variation seen in patients with BrS as well which serves as an arrhythmogenicity substrate by facilitating Phase 2 reentry. Previous studies have shown that a prolonged T_{PE} correlates with increased transmural repolarization heterogeneity.

Objective: To provide evidence based data supporting Hydroquinidine use to prevent life-threatening ventricular arrhythmia's in high risk patients with BrS.

Methods: Randomized, prospective multi-center, double blind study with two 18-month crossover phases (placebo and HQ groups) in high risk patients (N= 50) with BrS and an implanted ICD. HQ dose: 738±134mg/d
Primary Endpoints: Time to first appropriate ICD shock
Secondary Endpoints: Inappropriate shocks, ns VF/VT, death, SVT, syncope, HQ side effects.

Summary: There were no occurrences of ventricular arrhythmias among patients while receiving HQ, however statistical significance compared to placebo not observed due to lower than expected overall rate of arrhythmia and high treatment interruption (26%) due to dose-related side effects (mostly GI). One pt experienced arrhythmia while in placebo group and no patients experienced arrhythmia during treatment. Repolarization dispersion changes occurred promptly with acute HQ intake and maintained with chronic therapy which correlates with the clinical efficacy of HQ observed during electrical storms in BrS patients.

Table 3 Standard and repolarization dispersion ECG parameters measured before (Before HQ) and 3 hours after (Acute HQ) a 300-mg intake of hydroquinidine, under placebo, and with chronic HQ therapy

	Before HQ (n = 48)	Acute HQ (n = 48)	Placebo (n = 50)	Chronic HQ (n = 50)	*P* value
Standard ECG parameters					
Heart rate (bpm)	67 ± 10*	62 ± 10*†	68 ± 10	69 ± 10†	*.032; †.0004
PR (ms)	182 ± 31	185 ± 31	182 ± 36	186 ± 31	—
QRS (ms)	103 ± 17	104 ± 18	103 ± 17	103 ± 16	—
QT (ms)	387 ± 27*	414 ± 35*	388 ± 29†	411 ± 35†	*,†0.0001
QTc Bazett (ms)	404 ± 29*	417 ± 29*†	409 ± 32‡	433 ± 37†‡	*.027; †,‡<.0001
Max Jpoint elevation (mm)	1.6 ± 1.5	1.7 ± 1.6	1.8 ± 1.4	1.8 ± 1.5	—
Tpe (ms)					
V_1	79.3 ± 19.9	84.1 ± 24.5	69.7 ± 16.0*	77.4 ± 20.9*	*.0055
V_2	85.2 ± 19.4*	91.1 ± 25.0*	74.5 ± 16.8†	87.2 ± 21.5†	*.046; †<.0001
V_3	82.5 ± 15.2*	92.0 ± 18.8*	80.0 ± 17.1†	95.7 ± 29.5†	*.002; †<.0001
V_4	79.4 ± 15.7*	88.6 ± 20.5*	78.6 ± 13.8†	87.8 ± 25.1†	*.002; †.0013
V_5	76.6 ± 16.6*	87.2 ± 23.6*	75.4 ± 15.2†	83.8 ± 23.9†	*<.001; †.0028
V_6	73.4 ± 17.0*	83.4 ± 20.4*	69.5 ± 12.7†	79.0 ± 19.1†	*.001; †<.0001
Tpe/QTc					
V_1	0.205 ± 0.046	0.205 ± 0.046*	0.176 ± 0.040	0.181 ± 0.043*	.01
V_2	0.218 ± 0.032	0.218 ± 0.032	0.192 ± 0.040	0.208 ± 0.048	—
V_3	0.222 ± 0.037	0.222 ± 0.037	0.206 ± 0.046	0.225 ± 0.064	—
V_4	0.214 ± 0.036	0.214 ± 0.036	0.201 ± 0.033	0.207 ± 0.053	—
V_5	0.205 ± 0.039	0.214 ± 0.047*	0.193 ± 0.034	0.196 ± 0.048*	*.04
V_6	0.197 ± 0.040	0.209 ± 0.048*	0.180 ± 0.030	0.187 ± 0.038*	*.004
Tpe dispersion (ms)	31.0 ± 15.8	36.0 ± 19.0	29.6 ± 13.1*	42.3 ± 23.6*	*<.0001
Tpe max (ms)	94.8 ± 18.3*	106.6 ± 22.4*	89.4 ± 15.2†	107.7 ± 26.6†	*<.001; †<.0001

HQ-induced ECG changes were similar (except for QTc) regardless of daily dosage. HQ prolonged QT and QTc, and T_{PE} and T_{PE} max increased with no significant effects on J-point elevation, where as it was expected to decrease repolarization dispersion as its protective mechanism (refer to table 1).

Significance: HQ unexpected impact on T_{PE} suggests BrS involves both repolarization and depolarization abnormalities. HQ therapy may have a more complex role than simply a selective I_{to} blocking effect. This finding suggests that a global ionic effect of HQ may explain the variability in ECG modifications among studies. The difficulty in proving efficacy of HQ, high side effect profile and advancements in ICD devices supports the role for ICD placement as 1st line therapy for high risk patients. This study should not dissuade adjunct use of HQ for high risk patients with recurrent ventricular arrhythmias despite a not fully elucidated mechanism of action. Although statistical significant not obtained in this study, assuming it is efficient to prevent arrhythmia in BrS, its effect does not seem to be only and directly due to I_{to} inhibition.

Macrophages Facilitate Electrical Conduction in the Heart

Cell. April 20, 2017 169; 510-522.

Hulsmans M, Clauss S, Xiao L, Aguirre AD, King KR, Hanley A, Hucker WJ, Wülfers EM, Seemann G, Courties G, Iwamoto Y, Sun Y, Savol AJ, Sager HB, Lavine KJ, Fishbein GA, Capen DE, Da Silva N, Miquerol L, Wakimoto H, Seidman CE, Seidman JG, Sadreyev RI, Naxerova K, Mitchell RN, Brown D, Libby P, Weissleder R, Swirski FK, Kohl P, Vinegoni C, Milan DJ, Ellinor PT, Nahrendorf M.

Background:

Macrophages are cells typically known for their phagocytic properties and roles in adaptive immunity as well as wound healing. Over the past decade, however, there has been increased recognition of a subpopulation of 'resident' macrophages within all tissue types that perform novel, organ-specific roles. While macrophages have been previously documented within the myocardium and implicated in cardiac healing after injury, no study to date had documented a clear role for macrophages in the function of the cardiac conduction system. In this fascinating paper, Hulsmans *et al.* demonstrate the presence of tissue-resident macrophages in both murine and human AV nodes and implicate them in the maintenance of normal AV nodal conduction.

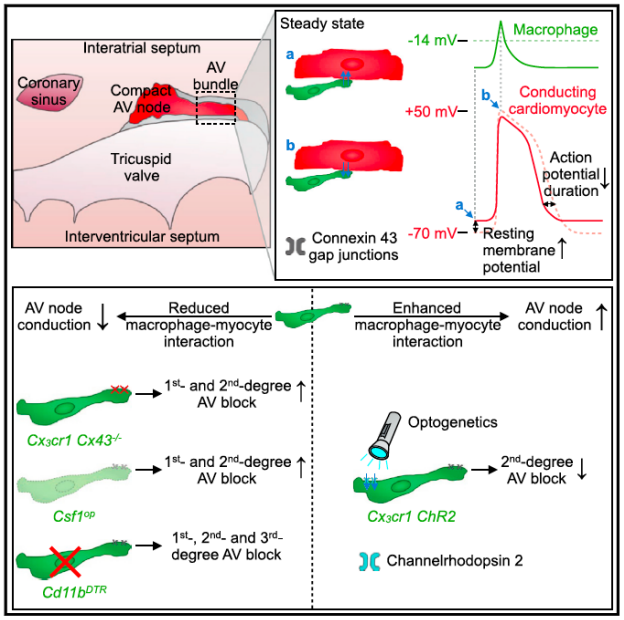

Graphical Abstract. ***Highlights:*** Tissue-resident macrophages are found in mice and human distal AV nodes. Macrophages are electrically coupled to surrounding cardiomyocytes by connexin 43. These resident macrophages modulate electrical activity of cardiomyocytes and, specifically, assist in normal AV nodal conduction.

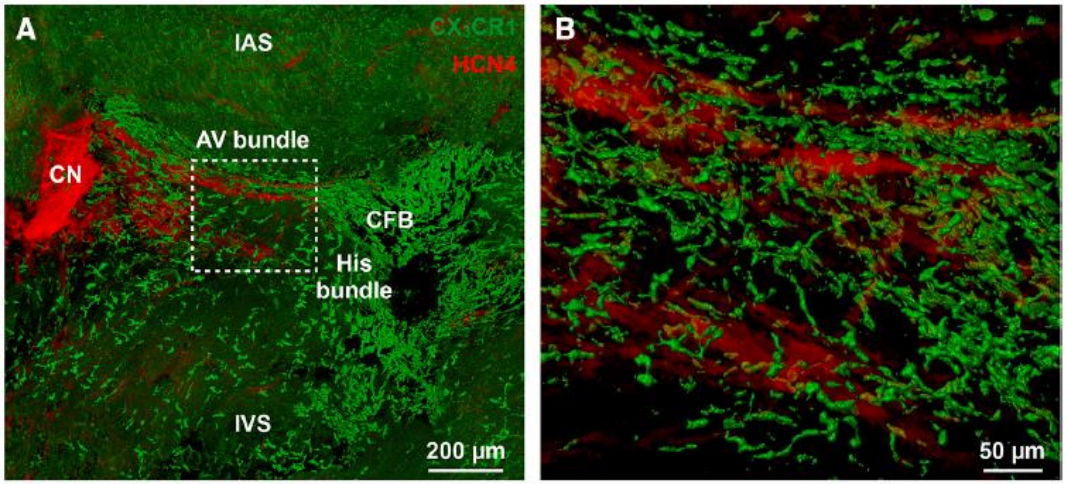

Figure 1A-B. Volumetric reconstruction of confocal microscopy after optical clearing of the AV node in a Cx3cr1$^{GFP/+}$ in which macrophages (green) constitutively expresss the green fluorescent protein (GFP) (**A**). The AV node (marked in red by staining for HCN4) is orientated along the AV groove, extending from the compact node (CN) into the proximal His bundle. Dashed square indicates the AV bundle. CFB, central fibrous body; IAS and IVS, interatrial and interventricular septum. (**B**) Higher magnification of dashed square in (**A**).

By: William Goodyer, MD/PhD

Summary:

First using the Cx3cr1$^{GFP/+}$ transgenic mouse line, in which the green fluorescent protein (GFP) is expressed within macrophages, the authors demonstrated that macrophages are present around all components of the cardiac conduction system (CCS), most notably surrounding the AV bundle (**Figure 1A-B**). Standard immunofluorescence staining coupled with optical clearing of human heart tissue confirmed the presence of macrophages surrounding human AV bundles, in addition to working myocardium. Further immunostaining and electron microscopy demonstrated that the points of contact between macrophages and cardiomyocytes were marked by the presence of connexin 43 (Cx43). Notably, whole-cell patch clamping showed that Cx43-containing gap junctions electrically coupled macrophages and conduction cells of the distal AV node (**Figure 4G-I**). Mathematical and computational modeling suggested that coupling increased numbers of macrophages to cardiomyocytes has the capacity to accelerate their repolarization. In an effort to show sufficiency of electric coupling between these cell types, they employed optogenetics to depolarize AV nodal macrophages on cue with light, which resulted in improved AV conduction. More convincingly, a series of three different genetic, loss-of-function mouse experiments demonstrated a necessity for cardiac macrophages (as well as for macrophage-specific Cx43-expression) in maintaining normal AV nodal function. The most pronounced phenotype came in Cd11b^{DTR} mice in which the diphtheria toxin receptor (DTR) was expressed within myeloid cells and thus allowed for efficient depletion of resident cardiac macrophages upon diphtheria exposure. While working cardiomyocytes remained unaffected in this *in vivo* model, severe depletion of cardiac macrophages resulted in progressive heart block, eventually evolving to third degree AV block (**Figure 7D**). Consistently, the severity of macrophage depletion correlated with the degree of heart block witnessed.

Significance:

In their paper, Hulsman *et al.* demonstrate a novel role for resident cardiac macrophages in the maintenance of normal atrioventricular conduction. Their findings provide a fresh avenue for investigation into the pathophysiology of AV nodal disease and heart block as well as possible novel therapeutic strategies via the modulation of macrophage function and coupling to cardiomyocytes. Notably, macrophage numbers and function have been previously shown to be altered following myocardial infarction and heart failure, disease processes frequently associated with arrhythmias. Given the presence of macrophages around other conduction cell types as well as the atrial and ventricular myocardium, further studies will need to be performed in order to investigate additional roles for macrophages as a previously unrecognized source of both atrial and ventricular dysrhythmias in various disease states.

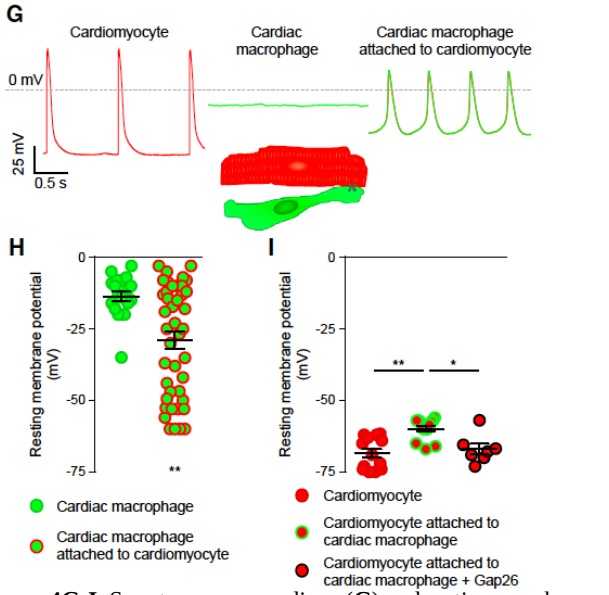

Figure 4G-I. Spontaneous recordings (**G**) and resting membrane potentials (**H**) by whole-cell patch clamp of solitary cardiac macrophages and macrophages attached to cardiomyocytes. Rhythmic depolarization was observed in 10/43 macrophages attached to CMs. (**I**) Resting membrane potential of solitary cardiomyocytes and cardiomyocytes coupled to macrophages before and after addition of the Cx43 inhibitor Gap26.

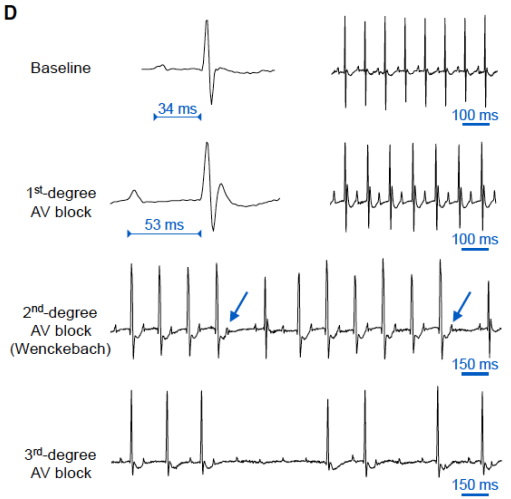

Figure 7D. ECG recordings before and after diphtheria toxin injection in Cd11b^{DTR} mice. Arrows indicate non-conducted P waves in second degree AV block.

Transient Notch Activation Induces Long-Term Gene Expression Changes Leading to Sick Sinus Syndrome in Mice

Circ Research. Aug 18;121(5):549-563.

Qiao Y, Lipovsky C, Hicks S, Bhatnagar S, Li G, Khandekar A, Guzy R, Woo KV, Nichols CG, Efimov IR, Rentschler S.

Background:

Notch signaling plays a crucial role in many aspects of normal cardiac development however it normally remains quiescent in healthy adult cardiomyocytes. Prior studies have shown that the Notch pathway is transiently re-activated in ventricles in response to injury, however no work to date had yet implicated Notch in *atrial* disease processes. Sick Sinus Syndrome (SSS) is a common and poorly understood syndrome encompassing a group of sinus rhythm disorders including inappropriate sinus bradycardia, frequent sinus pauses or arrest, and increased susceptibility to paroxysmal tachycardias such as atrial fibrillation. In this provocative study, *Qiao et al.* demonstrate transient Notch pathway re-activation in adult murine atrial cardiomyocytes occurs in response to injury. Further, ectopic activation of Notch in murine atria results in a phenotype reminiscent of SSS and is associated with gene expression changes that may provide potential insight into the underlying molecular mechanisms of this disease process.

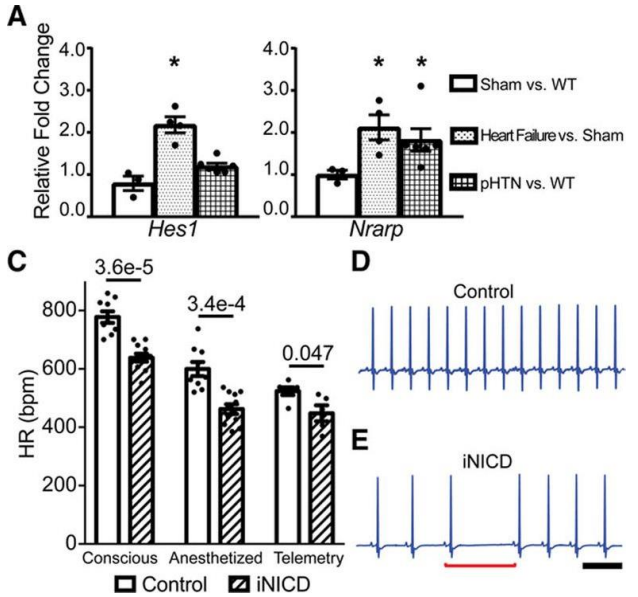

Figure 1A, C-E:.Notch signaling is reactivated in atria in mouse models of ischemic LV heart failure and pulmonary HTN **(A)**. Reverse transcriptase quantitative polymerase chain reaction (RT-qPCR) on right atrial (RA) samples showed elevated expression of Notch target genes including *Hes1* and *Nrarp* in both models of increased RA pressure **(A)**. *In vivo* overexpression of Notch signaling in adult mouse atria ("iNICD mice") resulted in decreased heart rates during both low and high activity periods **(C)**. Additionally, these iNICD mice exhibited an increased frequency of sinus pauses during telemetric monitoring **(D, E)**.

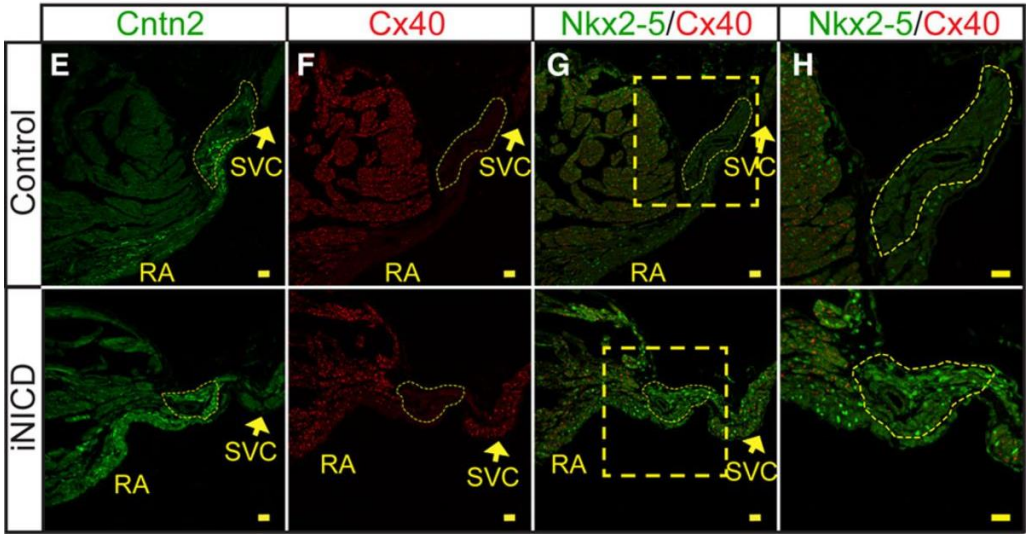

Figure 2E-H. *In vivo* overexpression of Notch signaling ("iNICD") in murine atria resulted in preserved SA nodal structure. The SAN was histologically identified as $Cntn2^{+}$ **(E)** and connexin 40^{-} ($Cx40^{-}$). **(F)**, myocardium at the junction of the SVC and RA. Yellow dashed lines demarcate the compact SAN, which had a similar morphology between control and iNICD mice. Notably, however, there was inappropriate mis-expression of Nkx2-5 (NK2 homeobox 5) in iNICD mice.

By: William Goodyer, MD/PhD

Summary:

Initially, the authors demonstrated unexpected Notch reactivation in atrial cardiomyocytes (CMs) within models of increased right atrial pressure, including ischemic LV heart failure and pulmonary HTN (**Figure 1**). Next, to further investigate the ramification of atrial Notch reactivation, they created a transgenic mouse strain in which the Notch intracellular domain could be induced within adult atrial cardiomyocytes (*"iNICD"* mice). Interestingly, this resulted in sinus bradycardia and an increased frequency of sinus pauses. While the SA node remained structurally intact with largely normal gene expression, there was inappropriate expression of *Nkx2-5*, a transcription factor normally expressed in atrial CMs and repressed in the SAN. Consistent with a more global atrial conduction defect, *in vivo* overexpression of Notch signaling within the SAN alone did not recapitulate the observed bradycardic phenotype. Also, using atrial activation maps, they demonstrated that the dominant pacemaker activity remained at the location of the SAN however the conduction velocity of atrial cardiomyocytes was slowed (**Figure 4**). Consistently, sharp microelectrode analysis of individual atrial cells in NICD mice revealed altered action potential dynamics, specifically a reduction in maximum upstroke velocity (**Figure 6**). Further molecular analysis revealed associated decreases in key atrial functional genes including *Scn5a* (which encodes the major *Na* channel of the heart), *Gja5 (Connexin 40)* (a major gap junction protein in atria) and *Tbx5* (**Figure 5**). Importantly, the authors demonstrated persistent phenotypes and gene expression changes despite only transient Notch activation. Finally, also consistent with a SSS-like phenotype, iNICD mice exhibited increased propensity for developing atrial dysrhythmias including atrial fibrillation.

Significance:

For the first time, Qiao *et al.* implicate Notch signaling in disordered atrial conduction. Specifically, they show that transient Notch reactivation within adult atrial cardiomyocytes resulted in profound and long-term atrial conduction defects, bradycardia, sinus pauses and increased susceptibility to atrial arrhythmias, together producing a phenotype resembling SSS. One caveat of the paper, however, remains that the iNICD mouse model represents an overexpression assay, making interpretation and extrapolation to human disease challenging. Additional correlation studies, including assessment of human atrial samples from patients with a history of SSS or right atrial stress (eg. PHTN) to assess for similar gene expression changes (eg. elevated *Hes1* and/or decreased *Scn5a* expression, etc.), could prove helpful in supporting their findings. More interestingly, in their injury models in which Notch signaling was reactivated (**Figure 1**), were similar atrial molecular and electrophysiologic changes observed as in their iNICD mice? If so, would blockade of Notch signaling alone prevent these damaging changes? While additional investigation is warranted, the findings by Qiao *et al.* provide fresh and exciting mechanistic insight into multiple atrial disease processes.

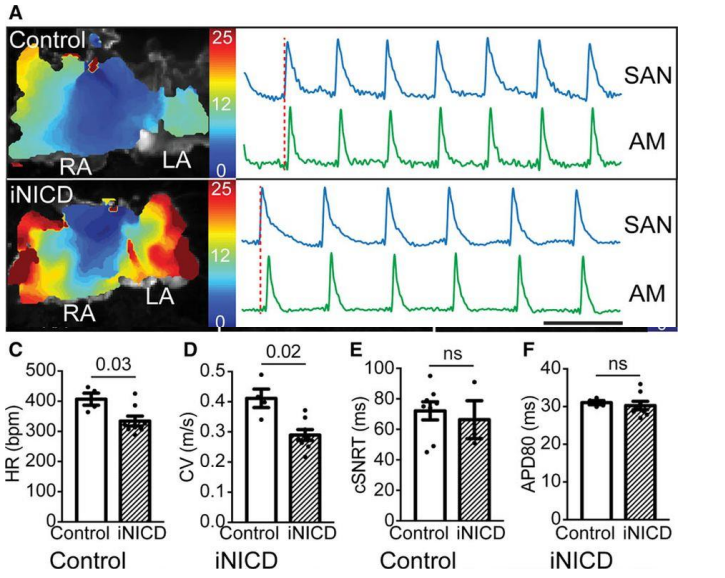

Figure 4A, C-F. Transient Notch activation resulted in stable slowing of atrial conduction velocity. Activation maps (**A, left**) from isolated atria in control and iNICD hearts during sinus rhythm demonstrate that despite a slower heart rate (**C**), the location of the dominant pacemaker remains the SAN in iNICD hearts. Optical action potentials (**A,** right) reveal 1:1 conduction between SAN and atria consistent with the absence of exit block. Slower conduction velocity (CV) (**D**) in iNICD mice when compared with controls, while the corrected SAN recovery time (cSNRT; **E**) and action potential duration at 80% repolarization (APD_{80}; **F**) remain unchanged.

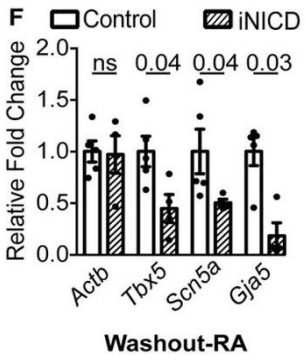

Figure 5F. Notch activation in atrial CMs reduced expression of several genes responsible for normal atrial function including Tbx5, Scn5a and Gja5.

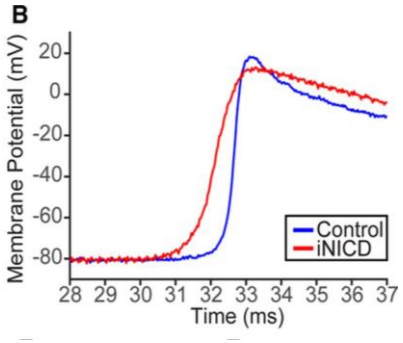

Figure 6B. Notch activation reduced atrial myocyte excitability. Individual action potentials from control (blue) and iNICD (red) RA cardiomyocytes recorded with sharp microelectrodes showed a reduction in maximum upstroke velocity (dV_m/dt_{max}).